



In-situ Synthesis and Macroscale Alignment of CsPbBr₃ Perovskite Nanorods in Polymer Matrix

Journal:	<i>Nanoscale</i>
Manuscript ID	NR-COM-06-2018-004895.R1
Article Type:	Communication
Date Submitted by the Author:	24-Jul-2018
Complete List of Authors:	<p>He, Juan; University of Central Florida, College of Optics and Photonics Towers, Andrew; University of Central Florida wang, yanan; Institute of Chemistry Yuan, Peisen; Changchun Institute of Applied Chemistry, Chinese Academy of Sciences Zhang, Jiang; Argonne National Lab, Advanced Photon Source Chen, Jiangshan; State Key Laboratory of Luminescent Materials and Devices, South China University of Technology Gesquiere, Andre; University of Central Florida, NanoScience Technology Center, Department of Chemistry and CREOL Wu , Shin-Tson ; University of Central Florida, College of Optics and Photonics Dong, Yajie; University of Central Florida, NanoScience Technology Center</p>



Journal Name

COMMUNICATION

In-situ Synthesis and Macroscale Alignment of CsPbBr₃ Perovskite Nanorods in Polymer Matrix

Received 00th January 20xx,
Accepted 00th January 20xx

Juan He, ‡^a Andrew Towers, ‡^{b,c} Yanan Wang, ‡^{b,#} Peisen Yuan,^d Zhang Jiang,^e Jiangshan Chen,^d
Andre J. Gesquiere,^{*a,b,c,f} Shin-Tson Wu,^{*a} and Yajie Dong,^{*a,b,f}

DOI: 10.1039/x0xx00000x

www.rsc.org/

We report an in-situ catalyst-free strategy to synthesize inorganic CsPbBr₃ perovskite nanorods in polymer matrix (NRs-PM) with good dimensional control, outstanding optical properties and ultrahigh environmental stability. Polarization photoluminescence (PL) imaging with high spatial resolution was carried out for the first time on single nanorod (NR) and shows relatively high local polarization ratio (~0.4) consistent with theoretical predictions based on a dielectric contrast model. We further demonstrate that macroscale alignment of the CsPbBr₃ nanorods can be achieved through mechanically stretching the NRs-PM films at elevated temperature, without deteriorating the optical quality of the NRs. A polarization ratio of 0.23 is observed for these aligned NRs-PM films, suggesting their potential as polarized down-converters to increase the light efficiency in liquid crystal display (LCD) backlights.

One dimensional (1D) semiconductor nanowires (NWs)¹⁻⁵ or nanorods (NRs)^{6,7} have long been considered as fundamental building blocks for nanoscience and technologies. Macroscale alignment of these building blocks could lead to functional structures or devices for electronics^{2,8}, photonics³, or optoelectronics^{4,9,10} applications. Aligned cadmium selenide (CdSe) based nanorods have been suggested for polarized light sources¹¹⁻¹⁸ which are of particular interests in liquid crystal display (LCD) back lighting¹⁹⁻²¹ for enhanced optical efficiency.

However, the relatively complicated synthetic process, high production cost and challenge of macroscale alignment have limited their adoption in display industry.^{22,23} A low cost, easy-to-align 1D luminescent nanomaterial system with polarized emission is thus highly desired.

Metal halide perovskites with a general formula of ABX₃, where A is methylammonium (MA), formamidinium (FA) or Cs; B is Pb or Sn; and X is Cl, Br, or I, have been under active investigation recently as promising low cost, high performance photovoltaic or light emitting materials.²⁴⁻³³ Among them, purely inorganic CsPbX₃ have been of special interests for their intrinsically higher stability compared to their organic-inorganic hybrid counterparts.³³⁻³⁶ Specifically, CsPbBr₃ has shown high emission efficiency and outstanding color purity,^{33,36,37} and 1D CsPbBr₃ nanostructures have demonstrated polarized emission³⁸⁻⁴⁰. Various synthetic methods have been investigated to achieve perovskite NWs/NRs, either in solution-phase⁴¹⁻⁵⁰ or vapor phase⁵¹ with considerable size and shape control and sometimes local alignment³⁸. However, macroscale alignment of CsPbBr₃ perovskite NW/NRs remains challenging. This is mainly because even with all-inorganic nanostructures, CsPbX₃ is still susceptible to heat and moisture.³⁸ Moreover, closely contacted NWs tend to aggregate and re-grow into bulk structures.⁴⁸

Here we report an in-situ catalyst-free strategy to synthesize CsPbBr₃ nanorods in polymer matrix (NRs-PM) with high stability that enables macroscale alignment without luminescence degradation.

The synthesis takes advantage of a simple swelling-deswelling microencapsulation (SDM) strategy recently demonstrated by our group.⁵² As schematically shown in Figure 1a, the CsPbBr₃ perovskite precursor solution was introduced into a polymer matrix (e.g. polystyrene) through solvent-induced swelling process and distributed in-between the swollen polymer chains as stripe-shaped droplets. Subsequently, in an annealing process, the solvent was driven out of the polymer matrix and perovskite nanocrystal nucleation initiated soon after solvent evaporated. This

^a College of Optics and Photonics, University of Central Florida, Orlando, Florida, USA. Email: yajie.dong@ucf.edu, swu@creol.ucf.edu, andre@ucf.edu

^b NanoScience Technology Center, University of Central Florida, Orlando, Florida, USA

^c Department of Chemistry, University of Central Florida, Orlando, Florida, USA

^d Institute of Polymer Optoelectronic Materials and Devices, State Key Laboratory of Luminescent Materials and Devices, South China University of Technology, Guangzhou, China

^e X-ray Science Division, Advanced Photon Source, Argonne National Laboratory, Argonne, Illinois, USA

^f Department of Materials Science & Engineering, University of Central Florida, Orlando, Florida, USA

[#] Present address: Laboratory of Advanced Optoelectronic Materials, College of Chemistry, Chemical Engineering and Materials Science, Soochow University, Suzhou 215123, China

† Electronic Supplementary Information (ESI) available. See DOI: 10.1039/x0xx00000x

‡ These authors contributed equally.

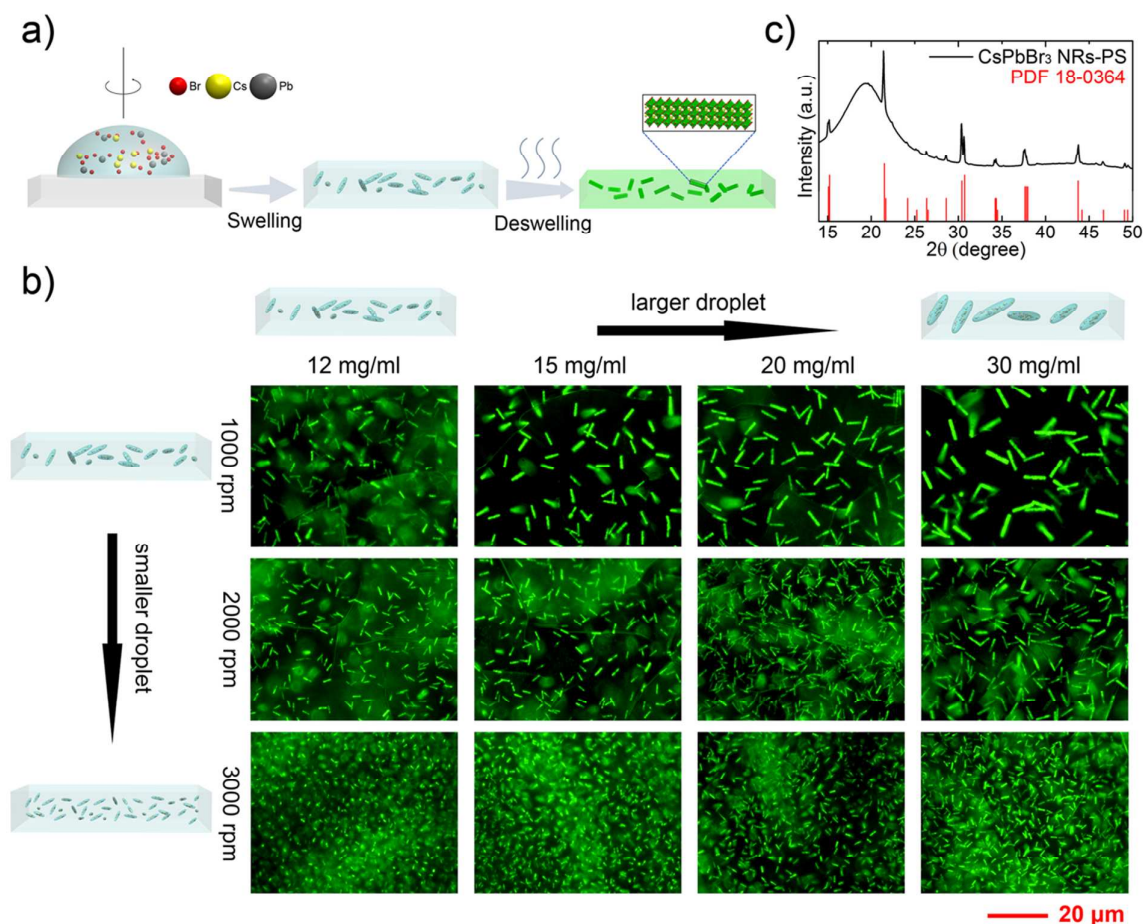


Figure 1 In-situ synthesis of luminescent CsPbBr₃ NRs-PM. (a) Scheme of CsPbBr₃ NRs-PM formation process through SDM. (b). Fluorescence microscopy images of NRs-PM synthesized with different precursor concentrations and different spincoating speeds. Focal planes were adjusted to be ~4-5 mm underneath the top surface for all samples. Insets on the top and left are schematic illustrations for droplet size under different conditions. (c) XRD pattern of CsPbBr₃ NRs-PS with standard monoclinic CsPbBr₃ (PDF 18-0364) as reference.

allowed precursors in droplets to reach supersaturation, which was followed by perovskite nanorod growth within the confinement of surrounding polymer chain clusters. Meanwhile, the polymer matrix deswelled and shrank, passivating and protecting the perovskite nanorods (Supporting experimental details).

In this system, the precursor content in each droplet has a direct effect on CsPbBr₃ NRs' size. It is therefore important to carefully monitor applied precursor concentration to achieve control of NR size. Considering the kinetics of precursor distribution in polymer matrix, lower precursor concentration leads to lower solution viscosity, which facilitates smaller droplets during the SDM process, thus generating smaller NRs. Increasing the rotational speed of the spin-coating process leads to more vigorous distribution of precursor droplets, also resulting in smaller droplet size thus smaller NRs.

Inspection of NRs in polystyrene matrix (NRs-PS) prepared with different precursor concentrations or spin-coating speeds with fluorescence microscopy (Figure 1b) clearly shows that NRs size can be reduced either by lowering precursor concentration or by increasing spin speed. The length of NRs can be tuned from as short as $1.27 \pm 0.16 \mu\text{m}$ obtained with 12

mg/ml CsPbBr₃ precursor at a speed of 3000 rpm to as long as $7.15 \pm 0.43 \mu\text{m}$ with 30 mg/ml precursor at 1000 rpm speed (Figure S1), with standard deviation no more than 12% and actually less than 9% in most of the conditions (Figure S2). The aspect ratios of the NRs synthesized at 1000 rpm/2000 rpm spin speed can be derived from the fluorescence microscopic images, with values ranging from 7.66 to 10.88 (Figure S3). It is also worth noting that these NRs are only observed with the microscope focal plane tuned to be several micrometers underneath the top surface, indicating good encapsulation with deswelled polymers.

XRD characterization was carried out to identify the crystal structure of the NRs-PM (Figure 1c). Although overlapped with the broad band polystyrene signal, clear sharp peaks from CsPbBr₃ NRs can be recognized, which match very well with the monoclinic structure of CsPbBr₃ (standard PDF card 18-0364). Lattice constant *a* and *c* were determined to be 5.84 Å and 5.88 Å, respectively.

Our in-situ SDM strategy is not limited to polystyrene substrates and appears to be a feasible synthesis strategy for most polymers that undergo a swelling-deswelling process when interacting with DMF solvent. In fact, fluorescent NR-

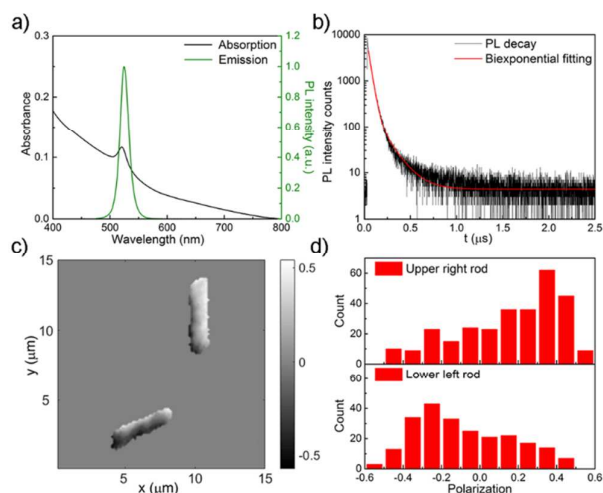


Figure 2 Optical properties of CsPbBr₃ NRs-PS. (a) UV-Vis absorption and PL spectra of NRs-PS (15mg/ml precursor, 2000 rpm). (b) PL decay (green) and corresponding fit (red) of NRs-PS. (c) Polarization map of NRs-PS. (d) Histograms of P (polarization) values obtained from the upper right rod (up) and lower left (down) rod in (c).

PMs were also obtained with other polymer substrates such as polycarbonate (PC) or acrylonitrile butadiene styrene (ABS) (Figure S4). The rod sizes are not identical for different polymers even when the same precursors and processing procedures were used. This is not surprising since the intrinsic polymer properties, such as swelling ratio in DMF solvent, polymer chain length and cluster morphology, etc., can vary for different polymers and may have a key impact on the dynamics of droplet distribution.

Figure 2a shows the absorption and photoluminescence (PL) spectra of typical NRs-PS samples, with absorption exciton peak at 520 nm and emission peak at around 526 nm. NRs-PS prepared at different conditions share the same exciton peak wavelength and only show different optical density with precursors of different concentrations (Figure S5). This result indicates that the rod size does not influence the optical properties too much, mainly because the NRs are in μm or sub- μm scale and the quantum confinement effect doesn't play an important role. Similarly, the PL emission peak is only slightly shifted within 2-3 nm range for samples with different processing conditions, as shown in Table S1. The narrow 18 nm full width at half maximum (FWHM) of the emission peak indicates excellent crystallinity and lack of defect states. Time-resolved PL decay of the NRs shows an average radiative lifetime τ_{avg} of ~ 50 ns, which is shorter than that observed for MAPbBr₃-PS (130 ns)⁵², as similarly noticed in reference³³. The NRs-PS films prepared under different conditions have photoluminescence quantum yield (PLQY) values ranging from 23% to 30% (Table S2).

For NRs, it is of great interest to see if their emission has some special properties with respect to their anisotropic shape. We therefore acquired single particle polarization PL

images of the NRs-PS using a home-built sample-scanning confocal microscope (Figure S6).

The sample was imaged over a $15 \times 15 \mu\text{m}^2$ area including two NRs. The intensities of two perpendicular polarized PL signals (I_x and I_y) were collected simultaneously (Figure S7). The resulting polarization P ($P=(I_y-I_x)/(I_y+I_x)$) image is shown in Figure 2c. The upper right rod which lies parallel to the y axis mostly shows positive P values, as illustrated in the upper histogram in Figure 2d, indicating that the PL emission is mostly polarized along the rod axis ($I_x < I_y$). On the other hand, the rod lying in nearly perpendicular direction in the lower left corner is mapped with more negative P value points (Figure 2d lower histogram), corresponding to $I_x > I_y$. This indicates that NRs with perpendicular orientations tend to cancel the PL polarization of each other, and thus macroscale NR alignment is necessary to avoid this polarization cancellation effect.

The origin of polarized emission of the CsPbBr₃ NRs-PS can be attributed to dielectric contrast between the NRs and the surrounding polymer matrix environment.⁵³ With the dielectric constants of CsPbBr₃ (6.35) and surrounding PS (2.6), the theoretical P of an infinitely long 1D nanostructure is calculated to be ~ 0.47 (Supporting Information). For NRs with a limited aspect ratio, it is reasonable to see that most of P values are lower than this limit. The P value of single NR could be further enhanced by increasing NRs' aspect ratio or using a polymer matrix with even lower dielectric constant.

The intimate passivation of the perovskite NRs by the surrounding polymer matrix yields great environmental stability even without further encapsulation. One as-obtained NRs-PS sheet with initial PLQY of 29% was cut into two pieces and placed in air and water respectively, with their luminescence periodically monitored. Interestingly, the NRs-PS became much brighter after being immersed in water for 277 days (Figure 3a). In fact, the PLQY increased to 40% within two weeks and then kept steady (Figure S8). The piece stored in air ended up with a PLQY of 31%.

Moisture enhanced PL in perovskite film has been reported before.⁵⁴⁻⁵⁹ The temporal PL enhancement was often attributed to reversible hydration and self-healing of the perovskite lattice by hydrogen bonding induced deactivation of nonradiative recombination centers.⁶⁰⁻⁶⁴ Such enhancement is usually observed in a relatively short period and further moisture exposure dissolves the perovskite materials and eventually leads to material decomposition and luminescence decay.⁶⁵ Here, with the intimate protection of PM matrix, a very limited amount of water molecules can penetrate inside to assist in the perovskite self-healing process over an extended period, yet doesn't appear to be able to induce perovskite dissolution. The absorption and PL spectra before and after the extended water immersion test did not change much except that the PL spectrum becomes slightly narrower (with FWHM decreased for 1nm) after water storage (Figure S9), which is attributed to healing of defects in the NRs and further confirms their outstanding long-term stability.

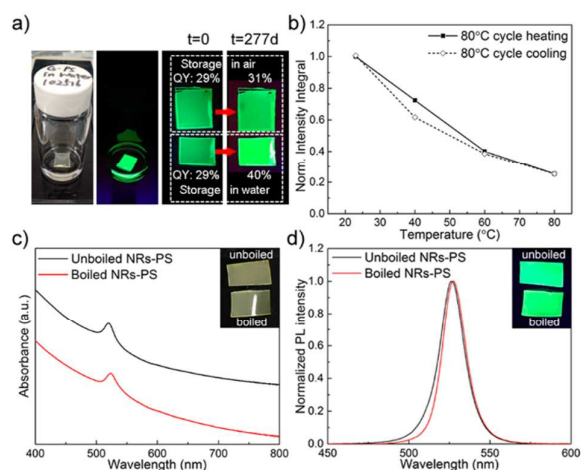


Figure 3 Water and thermal stability characterizations. (a) Photographs of CsPbBr₃ NRs-PS film immersed in water. From left to right: NRs-PS film stored in water bottle under ambient or UV illumination; Films brightness and PLQY at the beginning and after 277 days (top piece stored in air and bottom piece stored in water). (b) Temperature dependent PL of NRs-PS (c) Absorption and (d) PL emission spectra of the CsPbBr₃ NRs-PS film before (black) and after (red) boiling treatment.

Thermal stability was evaluated by heating up the NRs-PS film to 80°C, which is close to PS's glass transition temperature, and then cooling back to room temperature (RT). The NRs emission was quenched at higher temperature but could be fully recovered back at RT, as shown in Figure 3b. The absorption and PL emission spectra are identical before and after the heating process (Figure S10). To further test the performance under harsh treatment, half of the NRs-PS film was cut and put into boiling water (SI Video) for 30 seconds. Even though the boiled piece curved due to high temperature (Figure 3c inset), the boiled and unboiled samples showed similar luminescent brightness under UV illumination (Figure 3d inset). The absorption of the film remained unchanged after boiling (Figure 3c), while the PL spectrum narrowed (Figure 3d). As discussed above, heating treatment alone wouldn't induce such effect, so it is likely due to a water-assisted healing effect similar to that observed in the water-immersed sample but now accelerated by the higher temperature.

Water induced PL enhancement and healing effect was also observed for boiled NRs-PC sample and NRs-ABS sample stored in water for more than four months (NRs-ABS sample was not boiled because the glass transition temperature of ABS is lower than 100°C), as shown in Figure S11-14. This indicates the NRs-PM synthesized with our SDM strategy can generally benefit from such a healing effect to obtain better optical performance.

To utilize the above demonstrated polarized PL of the NR and avoid cancellation effect caused by random orientation distribution, macroscale alignment of these NRs is critical. The outstanding stability of the NRs-PM makes this feasible through simple mechanical stretching at elevated temperature. PS has a moderate glass transition temperature which allowed lab-testing of this concept. Being heated with a heat gun in air (Figure 4a), the NRs-PS film was steadily

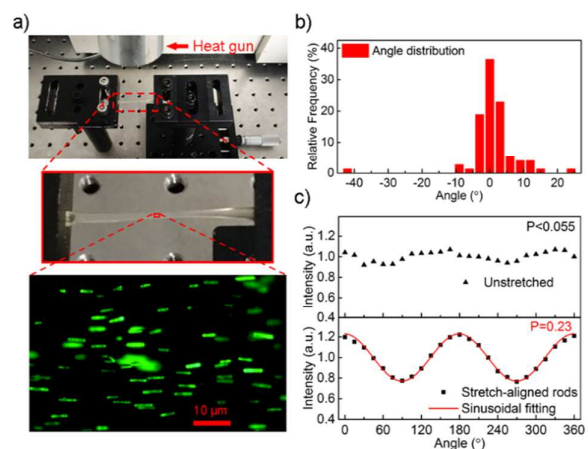


Figure 4 Stretch-alignment of CsPbBr₃ NRs-PS. (a) Up: setup for stretching the NRs-PS film; Middle: enlarged NRs-PS sample illustration; Down: Fluorescent microscopic image of stretch-aligned NRs. (b) Angle distribution of stretch-aligned NRs (in image a down). Elongation ratio is 8 to 1. (c) PL polarization of unstretched (up)/ stretch-aligned (down) NRs-PS.

stretched to a final length that is 8 times longer. Well aligned NRs were found with 37% of them lying in the $\pm 1.5^\circ$ range and 80% lying in $\pm 4.5^\circ$ range (Figure 4b) with respect to the stretching direction. Angle dependent PL intensity for NRs-PS samples was measured using the setup shown in Figure S15 and polarization P_s was derived from $P_s = (I_{max} - I_{min}) / (I_{max} + I_{min})$ (Figure 4c). The minor polarization of the NRs-PS film before stretching was attributed to uneven distribution of NR orientations. The PL angular dependence of the stretch-aligned NRs-PS complies well with a sinusoidal shape, with the maximum along the rod axis and the obtained highest P_s around 0.23. The polarization levels of stretch-aligned NRs-PS synthesized at different conditions are listed in Table S3, which are positively correlated to the aspect ratios of these NRs (Figure S16). As an average effect of polarized emission from all NRs, the polarization levels of these macroscale samples are consistent with the P value statistics obtained in single NR polarization PL imaging. Moreover, the polarized PL is almost independent from the polarization of the excitation laser beam (Figure S17).

We believe the process of stretching and aligning the NRs-PM film can easily be carried out in large scale given the maturity of industrial polymer processing techniques. With a polarization of 0.23, the aligned NRs-PM film can possibly improve the transmitted backlight in liquid crystal displays (LCD) from 50% to 62%.⁶⁶ Furthermore, the polarization level of aligned NRs can be improved by obtaining larger NR aspect ratio and using lower dielectric constant polymer material as matrix.

Conclusions

In summary, we demonstrate a simple and general strategy to achieve in-situ synthesis of stable, luminescent CsPbBr₃ perovskite NRs-PM with excellent emission color purity and size control. Polarized emission from single NR along the long

axis was observed in polarized PL imaging. Without further encapsulation, these NRs-PM demonstrated excellent water and thermal stability and can survive harsh treatment with retained or even enhanced luminescence efficiency. The NRs-PM can be easily aligned with good direction uniformity in macroscale and show polarized emission with a polarization value of 0.23. With further investigations and improvements in emission polarization, these perovskite NRs-PM could be promising building blocks for more efficient LCD backlight or other optical and photonic applications.

Conflicts of interest

There are no conflicts to declare.

Acknowledgements

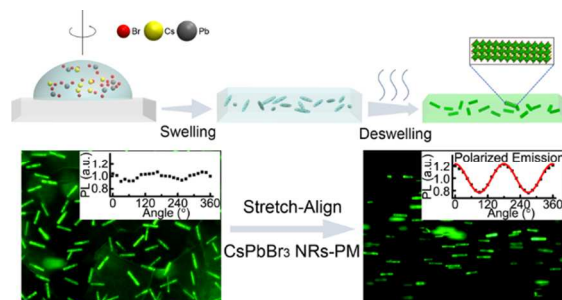
Y. Dong is grateful for support of this work by University of Central Florida through a startup funding (Grant No. 20080738). This research used resources of the Advanced Photon Source, a U.S. Department of Energy (DOE) Office of Science User Facility operated for the DOE Office of Science by Argonne National Laboratory under Contract No. DE-AC02-06CH11357. The authors thank Dr. Martin Schadt and Dr. Le Zhou for helpful discussion.

Notes and references

- 1 A. Zhang, G. Zheng and C. M. Lieber, *Nanowires: Building Blocks for Nanoscience and Nanotechnology*; Springer: New York, 2016.
- 2 W. Lu and C. M. Lieber, *Nat. Mater.*, 2007, **6**, 841.
- 3 R. Yan, D. Gargas and P. Yang, *Nat. Photonics*, 2009, **3**, 569.
- 4 Y. Li, F. Qian, J. Xiang and C. M. Lieber, *Mater. Today*, 2006, **9**, 18.
- 5 P. Yang, R. Yan and M. Fardy, *Nano Lett.* 2010, **10**, 1529.
- 6 A. P. Alivisatos, *Science*, 1996, **271**, 933.
- 7 X. Peng, L. Manna, W. Yang, J. Wickham, E. Scher, A. Kadavanich and A. P. Alivisatos, *Nature*, 2000, **404**, 59.
- 8 Y. Cui and C. M. Lieber, *Science*, 2001, **291**, 851.
- 9 X. Duan, Y. Huang, Y. Cui, J. Wang and C. M. Lieber, *Nature*, 2001, **409**, 66.
- 10 W. U. Huynh, J. J. Dittmer and A. P. Alivisatos, *Science*, 2002, **295**, 2425.
- 11 J. Hu, L. S. Li, W. Yang, L. Manna, L. W. Wang and A. P. Alivisatos, *Science*, 2001, **292**, 2060.
- 12 C. X. Shan, Z. Liu and S. K. Hark, *Phys. Rev. B: Condens. Matter Mater.*, 2006, **74**, 8.
- 13 I. Hadar, G. B. Hitin, A. Sitt, A. Faust and U. Banin, *J. Phys. Chem. Lett.*, 2013, **4**, 502.
- 14 A. Sitt, A. Salant, G. Menagen and U. Banin, *Nano Lett.*, 2011, **11**, 2054.
- 15 D. V. Talapin, R. Koeppel, S. Götzinger, A. Kornowski, J. M. Lupton, A. L. Rogach, O. Benson, J. Feldmann and H. Weller, *Nano Lett.*, 2003, **3**, 1677.
- 16 I. Hadar, J. P. Philbin, Y. E. Panfil, S. Neyshtadt, I. Lieberman, H. Eshet, S. Lazar, E. Rabani and U. Banin, *Nano Lett.*, 2017, **17**, 2524.
- 17 G. Yang, H. Zhong, Z. Bai, R. Liu and B. Zou, *Adv. Opt. Mater.*, 2014, **2**, 885.
- 18 Y. Gao, V. D. Ta, X. Zhao, Y. Wang, R. Chen, E. Mutlugun, K. E. Fong, S. T. Tan, C. Dang, X. W. Sun, H. Sun and H. V. Demir, *Nanoscale*, 2015, **7**, 6481.
- 19 A. K. Srivastava, W. Zhang, J. Schneider, A. L. Rogach, V. G. Chigrinov and H. S. Kwok, *Adv. Mater.*, 2017, **29**, 1701091.
- 20 K. Neyts, M. Mohammadimasoudi, Z. Hens and J. Beeckman, *SID Symp. Dig. Tech. Papers*, 2016, **47**, 552.
- 21 P. D. Cunningham, J. B. Souza Jr, I. Fedin, C. She, B. Lee and D. V. Talapin, *ACS Nano*, 2016, **10**, 5769.
- 22 M. Hasegawa, Y. Hirayama and S. Dertinger, *SID Symp. Dig. Tech. Papers*, 2015, **46**, 67.
- 23 M. Hasegawa and Y. Hirayama, *SID Symp. Dig. Tech. Papers*, 2016, **47**, 241.
- 24 D. Bi, W. Tress, M. I. Dar, P. Gao, J. Luo, C. Renevier, K. Schenk, A. Abate, F. Giordano, J. P. C. Baena and J. D. Decoppet, *Sci. Adv.* 2016, **2**, e1501170.
- 25 B. Luo, Y. C. Pu, S. A. Lindley, Y. Yang, L. Lu, Y. Li, X. Li and J. Z. Zhang, *Angewandte Chemie Int. Ed.*, 2016, **55**, 8864.
- 26 H. Cho, S. H. Jeong, M. H. Park, Y. H. Kim, C. Wolf, C. L. Lee, J. H. Heo, A. Sadhanala, N. Myoung, S. Yoo and S. H. Im, *Science*, 2015, **350**, 1222.
- 27 S. D.; Stranks and H. J. Snaith, *Nat. Nanotechnol.*, 2015, **10**, 391.
- 28 L. Zhang, X. Yang, Q. Jiang, P. Wang, Z. Yin, X. Zhang, H. Tan, Y. M. Yang, M. Wei, B. R. Sutherland and E. H. Sargent, *Nat. Commun.*, 2017, **8**, 15640.
- 29 S. A. Veldhuis, P. P. Boix, N. Yantara, M. Li, T. C. Sum, N. Mathews and S. G. Mhaisalkar, *Adv. Mater.*, 2016, **28**, 6804.
- 30 M. A. Green, A. Ho-Baillie and H. J. Snaith, *Nat. Photonics*, 2014, **8**, 506.
- 31 X. He, Y. Qiu and S. Yang, *Adv. Mater.* 2017, **29**, 1700775.
- 32 Q. Zhou, Z. Bai, W. G. Lu, Y. Wang, B. Zou and H. Zhong, *Adv. Mater.*, 2016, **28**, 9163.
- 33 L. Protesescu, S. Yakunin, M. I. Bodnarchuk, F. Krieg, R. Caputo, C. H. Hendon, R. X. Yang, A. Walsh and M. V. Kovalenko, *Nano Lett.*, 2015, **15**, 3692.
- 34 Y. Wang, X. Li, J. Song, L. Xiao, H. Zeng and H. Sun, *Adv. Mater.*, 2015, **27**, 7101.
- 35 M. Kulbak, D. Cahen and G. Hodes, *J. Phys. Chem. Lett.*, 2015, **6**, 2452.
- 36 A. Swarnkar, R. Chulliyil, V. K. Ravi, M. Irfanullah, A. Chowdhury and A. Nag, *Angew. Chem. Int. Ed.*, 2015, **127**, 15644.
- 37 X. Li, Y. Wu, S. Zhang, B. Cai, Y. Gu, J. Song and H. Zeng, *Adv. Funct. Mater.*, 2016, **231**, 2435.
- 38 S. N. Raja, Y. Bekenstein, M. A. Koc, S. Fischer, D. Zhang, L. Lin, R. O. Ritchie, P. Yang and A. P. Alivisatos, *ACS Appl. Mater. Interfaces*, 2016, **8**, 35523.
- 39 W. G. Lu, X. G. Wu, S. Huang, L. Wang, Q. Zhou, B. Zou, H. Zhong and Y. Wang, *Adv. Opt. Mater.*, 2017, **5**, 1700594.
- 40 D. Wang, D. Wu, D. Dong, W. Chen, J. Hao, J. Qin, B. Xu, K. Wang and X. Sun, *Nanoscale*, 2016, **8**, 11565.
- 41 Y. Fu, H. Zhu, C. C. Stoumpos, Q. Ding, J. Wang, M. G. Kanatzidis, X. Zhu and S. Jin, *ACS Nano*, 2016, **10**, 7963.
- 42 H. Zhu, Y. Fu, F. Meng, X. Wu, Z. Gong, Q. Ding, M. V. Gustafsson, M. T. Trinh, S. Jin and X. Y. Zhu, *Nat. Mater.*, 2015, **14**, 636.
- 43 S. W. Eaton, M. Lai, N. A. Gibson, A. B. Wong, L. Dou, J. Ma, L. W. Wang, S. R. Leone and P. Yang, *Proc. Natl. Acad. Sci.*, 2016, **113**, 1993.
- 44 P. Zhu, S. Gu, X. Shen, N. Xu, Y. Tan, S. Zhuang, Y. Deng, Z. Lu, Z. Wang and J. Zhu, *Nano Lett.*, 2016, **16**, 871.
- 45 H. Deng, D. Dong, K. Qiao, L. Bu, B. Li, D. Yang, H. E. Wang, Y. Cheng, Z. Zhao, J. Tang and H. Song, *Nanoscale*, 2015, **7**, 4163.
- 46 A. B. Wong, M. Lai, S. W. Eaton, Y. Yu, E. Lin, L. Dou, A. Fu and P. Yang, *Nano Lett.*, 2015, **15**, 5519.

- 47 D. Zhang, S. W. Eaton, Y. Yu, L. Dou and P. Yang, *J. Am. Chem. Soc.* 2015, **137**, 9230.
- 48 M. J. Ashley, M. N. O'Brien, K. R. Hedderick, J. A. Mason, M. B. Ross and C. A. Mirkin, *J. Am. Chem. Soc.* 2016, **138**, 10096.
- 49 S. Sun, D. Yuan, Y. Xu, A. Wang and Z. Deng, *ACS Nano*, 2016, **10**, 3648.
- 50 L. Dou, M. Lai, C. S. Kley, Y. Yang, C. G. Bischak, D. Zhang, S. W. Eaton, N. S. Ginsberg and P. Yang, *Proc. Natl. Acad. Sci.*, 2017, **114**, 7216.
- 51 J. Xing, X. F. Liu, Q. Zhang, S. T. Ha, Y. W. Yuan, C. Shen, T. C. Sum and Q. Xiong, *Nano Lett.*, 2015, **15**, 4571.
- 52 Y. Wang, J. He, H. Chen, J. Chen, R. Zhu, P. Ma, A. Towers, Y. Lin, A. J. Gesquiere, S. T. Wu and Y. Dong, *Adv. Mater.*, 2016, **28**, 10710.
- 53 J. Wang, M. S. Gudixsen, X. Duan, Y. Cui and C. M. Lieber, *Science*, 2001, **293**, 1455.
- 54 G. E. Eperon, S. N. Habisreutinger, T. Leijtens, B. J. Bruijnaers, J. J. van Franeker, D. W. deQuilettes, S. Pathak, R. J. Sutton, G. Grancini, D. S. Ginger, R. A. Janssen, A. Petrozza and H. J. Snaith, *ACS Nano*, 2015, **9**, 9380.
- 55 W. Zhou, Y. Zhao, C. Shi, H. Huang, J. Wei, R. Fu, K. Liu, D. Yu and Q. Zhao, *J. Phys. Chem. C*, 2016, **120**, 4759.
- 56 X. Gong, M. Li, X. B. Shi, H. Ma, Z. K. Wang and L. S. Liao, *Adv. Funct. Mater.*, 2015, **25**, 6671.
- 57 J. You, Y. Yang, Z. Hong, T. B. Song, L. Meng, Y. Liu, C. Jiang, H. Zhou, W. H. Chang, G. Li and Y. Yang, *Appl. Phys. Lett.*, 2014, **105**, 183902.
- 58 Z. Zhu, V. G. Hadjiev, Y. Rong, R. Guo, B. Cao, Z. Tang, F. Qin, Y. Li, Y. Wang, F. Hao and S. Venkatesan, *Chem. Mater.*, 2016, **28**, 7385.
- 59 S. G. R. Bade, J. Li, X. Shan, Y. Ling, Y. Tian, T. Dilbeck, T. Besara, T. Geske, H. Gao, B. Ma and K. Hanson, *ACS Nano*, 2016, **10**, 1795.
- 60 X. Zhang, X. Bai, H. Wu, X. Zhang, C. Sun, Y. Zhang, W. Zhang, W. Zheng, W. W. Yu and A. L. Rogach, *Angew. Chem. Int. Ed.*, 2018, **57**, 3337.
- 61 K. K. Bass, R. E. McAnally, S. Zhou, P. I. Djurovich, M. E. Thompson and B. C. Melot, *Chem. Commun.*, 2014, **50**, 15819.
- 62 C.-H. Chiang, M. K. Nazeeruddin, M. Gratzel and C.-G. Wu, *Energy Environ. Sci.*, 2017, **10**, 808.
- 63 R. L. Z. Hoye, M. R. Chua, K. P. Musselman, G. Li, M.-L. Lai, Z.-K. Tan, N. C. Greenham, J. L. MacManus-Driscoll, R. H. Friend and D. Credgington, *Adv. Mater.*, 2015, **27**, 1414.
- 64 A. M. Leguy, Y. Hu, M. Campoy-Quiles, M. I. Alonso, O. J. Weber, P. Azarhoosh, M. Van Schilfgaarde, M. T. Weller, T. Bein, J. Nelson and P. Docampo, *Chem. Mater.*, 2015, **27**, 3397.
- 65 J. M. Frost, K. T. Butler, F. Brivio, C. H. Hendon, M. Van Schilfgaarde and A. Walsh, *Nano Lett.*, 2014, **14**, 2584.
- 66 J. He, Y. Wang, H. Chen, A. Towers, P. Yuan, Z. Jiang, C. Zhang, J. Chen, A. J. Gesquiere, S. T. Wu and Y. Dong, *SID Symp. Dig. Tech. Papers*, 2018, **49**, 218.

SYNOPSIS Table of Contents Graphic.



Stretch-alignment of CsPbBr₃ perovskite nanorods synthesized in-situ in polymer matrix leads to polarized emission.